

Cutting Parameter Optimization based on Online Temperature Measurements

Abdelillah Djamal Kara Ali

Department of Mechanical Engineering, University of Tlemcen, Algeria
dj_kara_ali@yahoo.fr
(corresponding author)

Nasreddine Benhadji Serradj

Department of Mechanical Engineering, University of Tlemcen, Algeria
kawther4499@yahoo.fr

Mohamed El Amine Ghernaout

Department of Mechanical Engineering, University of Tlemcen, Algeria
e_amine2001@yahoo.fr

Received: 20 September 2022 | Revised: 26 October 2022 | Accepted: 27 October 2022

ABSTRACT

The deformation of metallic materials during the machining operation requires a significant amount of energy. During the chip formation process and due to the plastic deformation of the metal and the friction along the tool-part interface, the thermal loads generated are strongly impacted by the cutting factors. Thus, the choice of optimized cutting conditions is essential to control the quality of the work required. The aim of the present experimental study is to optimize the cutting parameters using temperature measurements. The average temperature of the cutting tool is studied using a FLIR A325sc type infrared camera. Optimal cutting parameters for each performance metric were obtained using the Taguchi techniques.

Keywords-machining; cutting conditions; optimization; thermography; temperature measurement

I. INTRODUCTION

The choice of cutting conditions is a very important factor in machining. With the increasingly rapid development of machine tools and the use of new high-performance materials for the tool-part couple, cutting temperature is an essential concern in machining. To be highly competitive, the objectives sought by the mechanical manufacturing industries are to produce high quality products with low cost and time constraints. To achieve them, one of the solutions is to optimize machining parameters such as cutting speed, depth of cut and feed. The effects of cutting parameters (cutting speed, depth of cut, feed per revolution,) on surface roughness, tool wear, cutting forces related to turning operations have been studied in depth. Authors in [1] used the Response Surface Method (RSM) with a factorial design to predict surface roughness when machining high strength materials. Authors in [2] studied the machinability of hard steel in turning by the response surface method. Authors in [3] used a multiplicative model to predict surface roughness and tool vibration. The context of the current work is based on the use of full factorial type experimental designs based on the experimental characterization of the temperature measurement for the

optimization of the cutting conditions during the turning operation. Many techniques have been developed during the recent years that address this type of problem. Authors in [4] propose a general classification of the different techniques for modeling and optimizing input-output relationships in metal cutting processes. They are classified into two methods, classical optimization techniques and unconventional techniques. The current work is oriented on the study of the heat flow in the zone of the cut represented by the measurement of the temperature. Various techniques of temperature measurement have been studied and evaluated [5-8]. The optical infrared method has been used in [9-10].

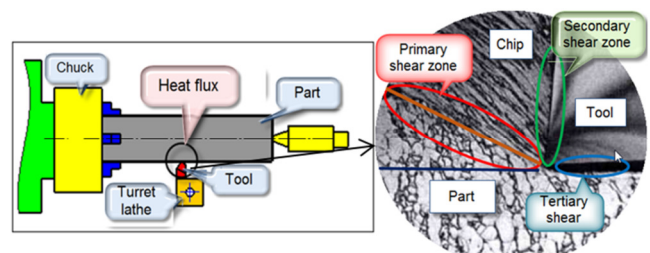


Fig. 1. Sources of heat generation in machining.

At the heart of the process, two main phenomena are in interaction:

- A very strong plastic deformation in the shear zones.
- The friction of the chip on the rake face of the tool.

One may also add the friction of the clearance face on the newly machined surface. The energy generated is then largely transformed into a significant heat flux which modifies and deteriorates the machined surface and the cutting tool shown in Figure 1.

In this paper, an experimental measurement methodology is proposed and the results are presented using an acquisition instrumentation, equipped with a single infrared camera with advantages such as contactless measurement, measurement without or with very little disturbance between the surface of the studied object and its surrounding environment, the capacity for real-time measurement, wide range of operating temperatures, the ability to adapt to any type of material, and a unit processing of the measured values. The correlation between the cutting conditions and the temperature appears on the flowchart represented in Figure 2.

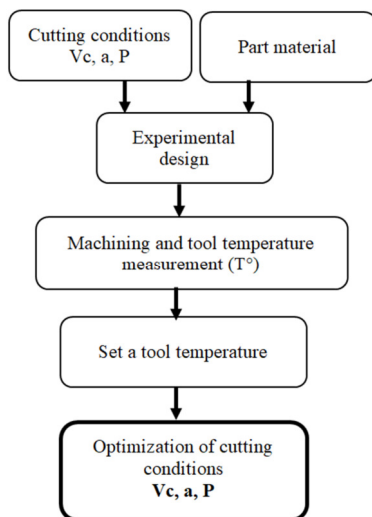


Fig. 2. Correlation between cutting conditions and temperature.

In industry and in order to make the best choices, very often one empirical method (Taylor's law, Kronenberg model, etc.) is used to calculate and optimize the cutting parameters before machining. Knowing that the low cumulative gains generate significant profits, we propose an approach that allows refining the manufacturing conditions after following the experimental tests.

II. MATERIALS AND METHODS

The infrared camera used is the Flir A325sc, coupled with the FLIR Research software. The inserts are made of tungsten carbide with a beak radius $r = 0.4\text{mm}$ (Figure 3). The specimens are made of S185 steel, a material widely used in industry. For the machining we used a conventional parallel lathe made by TOS TRENCIN type (Figure 4).



Fig. 3. Thermal camera FLIR A325sc and tool holder with the used insert.



Fig. 4. Machining station with tool, specimen, and camera.

The conducted experimental tests and the calibration of the camera are widely discussed in [11]. Before using the results, the data are retrieved from the camera software (FLIR Quick Plot) for viewing the machining sequences. Figure 5 represents the acquisition chain.



Fig. 5. Chain of acquisition and processing of thermal data.

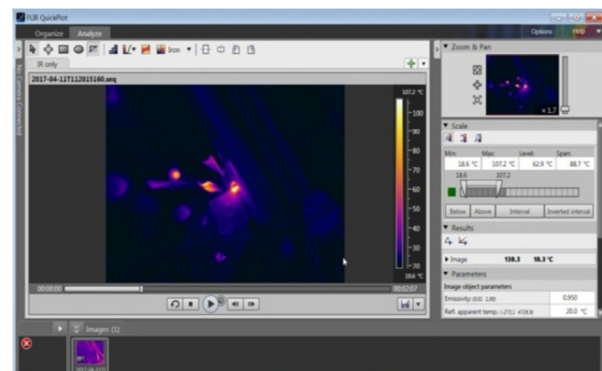


Fig. 6. Software interface.

The recovery of the temperatures is made after tracing the curve represented by Figure 7. The curve is divided into three zones:

- Zone 1 represents the machining initiation.

- Zone 2 determines the stabilization part of the section, from the latter we recover the temperatures for analysis.
- Zone 3 represents the tool release and the end of the turning operation.

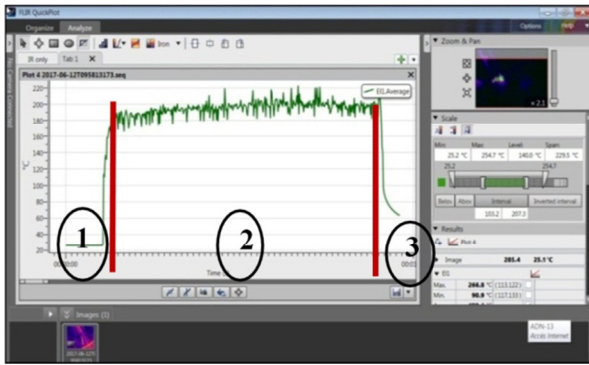


Fig. 7. Software interface and curve areas studied.

III. TEMPERATURE PREDICTION MODEL

The relationship between the inputs which are the machining parameters (cutting speed, feed, depth of cut) as independent variables vary according to an N³ type design of experiments. In a 4³ type experiment, each parameter has 4 levels, which gives us 64 experiments (full plan). We carried out 64 machining operations, each time using a new cutting edge. The expanded linear model of the type second-order equation is:

$$Y = b_0 + b_1X_1 + b_2X_2 + b_3X_3 + b_{11}X_1^2 + b_{22}X_2^2 + b_{33}X_3^2 + b_{12}X_1X_2 + b_{13}X_1X_3 + b_{23}X_2X_3 \quad (1)$$

where Y = T is the estimated response, X₁, X₂, X₃ respectively represent the control factors (cutting speed, feed, and depth of cut), and b₀, ..., b₂₃ are the coefficients of the related factors. Constants and exponents are determined by the least squares method. After careful reading of the sequences recorded by the camera, we determined the temperature of the tip of the tool according to the cutting parameters as shown in Table I.

TABLE I. CUTTING PARAMETERS

Parameter	Code	Levels			
		1	2	3	4
Cutting speed Vc (m/min)	X ₁	78	112	157	220
Feed rate a (mm/rev)	X ₂	0.08	0.11	0.14	0.20
Depth of cut P (mm)	X ₃	0.25	0.5	0.75	1
Turning conditions	Machining without lubrication				

The analysis of variance in Table II shows that the interaction feed and depth of cut clearly influence the temperature (P-value =0.04). After processing, we obtain the prediction equation (2):

$$T^{\circ} \text{ tool} = 89.6 + 0.054 Vc - 638 a - 19.2 P - 0.000215 Vc^2 + 1640 a^2 + 32.3 P^2 + 0.572 Vcxa + 0.036 VcxP + 368 axP \quad (2)$$

The residual distribution analysis is based on a powerful test for the detection of non-normality. The normal probability plot is shown in Figure 8. It is clear that the residuals lie close

to the reference line, which implies that the errors are normally distributed.

TABLE II. ANALYSIS OF VARIANCE

Source	DF	Adj SS	Adj MS	F-value	P-value
Regression	9	34124.1	3791.57	12.63	0.000
Vc	1	8.0	7.95	0.03	0.871
a	1	677.8	677.83	2.26	0.139
P	1	38.2	38.18	0.13	0.723
VcxVc	1	14.4	14.39	0.05	0.828
axa	1	438.5	438.46	1.46	0.232
PxP	1	260.5	260.46	0.87	0.356
Vcxa	1	116.4	116.40	0.39	0.536
VcxP	1	17.9	17.85	0.06	0.808
axP	1	1333.7	1333.65	4.44	0.040
Error	54	16212.6	300.23		
Total	63	50336.7			

TABLE III. COEFFICIENTS OF EQUATION (2)

Term	Coef	SE Coef	T-value	P-value	VIF
Constant	89.6	43.3	2.07	0.043	
Vc	0.054	0.335	0.16	0.871	67.55
a	-638	424	-1.50	0.139	75.61
P	-19.2	53.8	-0.36	0.723	48.28
VcxVc	-0.000215	0.000982	-0.22	0.828	53.63
axa	1640	1357	1.21	0.232	63.50
PxP	32.3	34.7	0.93	0.356	32.25
Vcxa	0.572	0.918	0.62	0.536	17.03
VcxP	0.036	0.146	0.24	0.808	13.11
axP	368	175	2.11	0.040	14.92

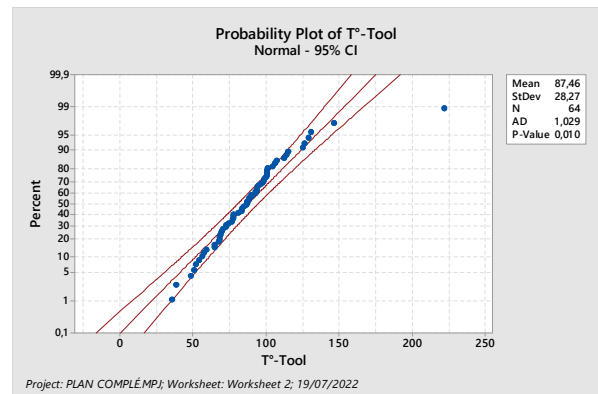


Fig. 8. Normality line of the distribution of residuals.

IV. RESULTS AND DISCUSSION

The test results were divided according to the method of measurement, either in zone 2 or zone 3. The results obtained during the first method (zone 2) have been discussed in [12]. We present the results obtained in zone 3 where the temperature measurement is made just after the release of the tool. The comparison between the experimental values and the predicted values for the obtained temperature model, is represented graphically in Figure 9 for the complete design of the experiment. The latter shows that the experimental and the estimated values are close with an accuracy of 88.87%. These results prove the accuracy of the model. Furthermore, they confirm that the model can be effectively used to predict the machining temperature with a 95% confidence interval.

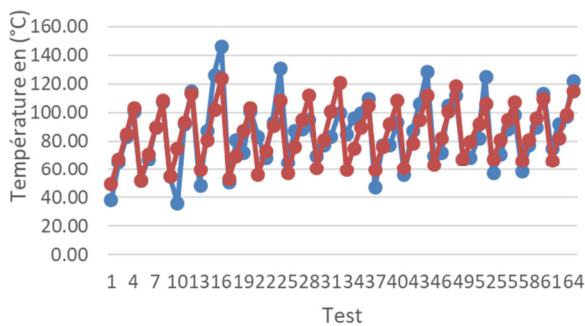


Fig. 9. Experimental and predicted curves.

Figure 10 shows the different interactions. The interaction $V_c \times p$ (between the cutting speed and the depth of cut) is noticed to have an imposing effect. On the other hand, the interaction $a \times p$ (between the feed and the depth of cut) and the interaction $V_c \times a$ (between cutting speed and feed) are less significant. Most of the energy released is spent in deforming the chips both cutting and plastically. Part of this energy is transformed into heat by friction at the two interfaces (tool-chip and tool-workpiece). The generation of heat during machining causes the temperature to rise in the process area. It turns out that the cutting speed is the imposing factor on the cutting temperature. To visualize the influence of the cutting parameters on the temperature (T°), the response surfaces (2D) are presented below.

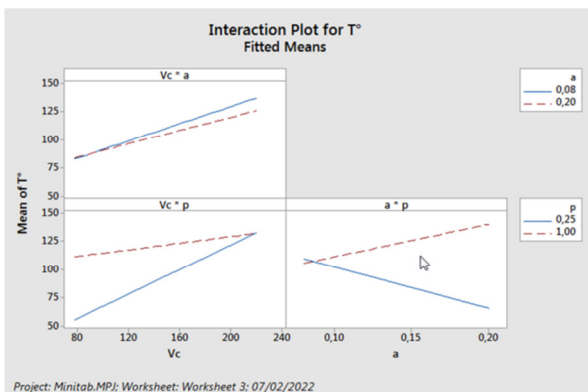


Fig. 10. Interactions of cutting conditions.

The isotherm in Figure 11 shows that the cutting temperature increases with the feed over the interval of 0.08mm/rev and 0.14mm/rev, with a drop in temperature over the interval 0.14mm/rev and 0.2mm/rev. The thermogram in Figure 12 shows the concentration of heat on the tool tip and chip fragments. The isotherm in Figure 13 shows that the cutting temperature increases with increasing cutting speed and depth of cut. The thermogram in Figure 14 shows the heat distribution on the cut face. The isotherm in Figure 15 shows that the temperature increases for the interval of the feed rate (0.14mm/rev-0.2mm/rev) and the depth of cut (0.75mm-1mm) and it remains moderate for the lower intervals. As can be seen, for a depth of cut equal to 0.25mm, the temperature decreases. The thermogram in Figure 16 shows the concentration of heat on the nose of the tool.

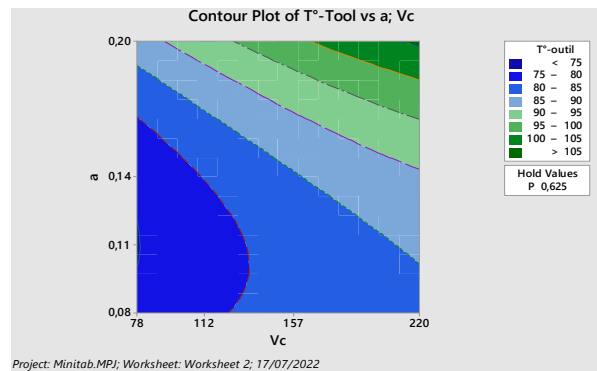


Fig. 11. Temperature isotherm as a function of cutting speed and feed rate.



Fig. 12. Thermogram for $V_c=78\text{m/min}$, $a=0.08\text{mm/rev}$, and $P=0.25\text{mm}$.

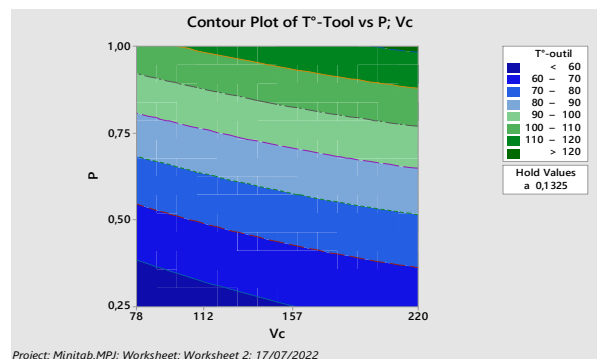


Fig. 13. Isotherm as a function of cutting speed and depth of cut.



Fig. 14. Thermogram for $V_c=157\text{m/min}$, $a=0.08\text{mm/rev}$, and $P=0.75\text{ mm}$.

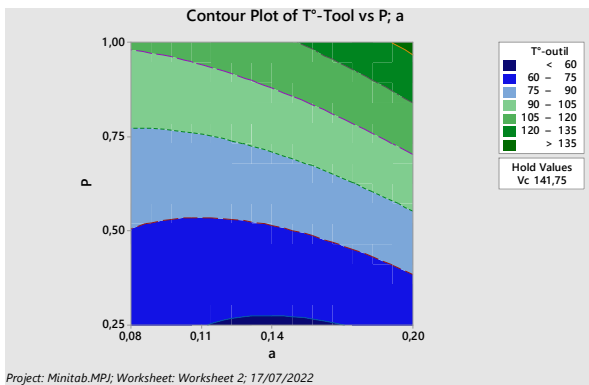


Fig. 15. Isotherm as a function of feed rate and depth of cut.

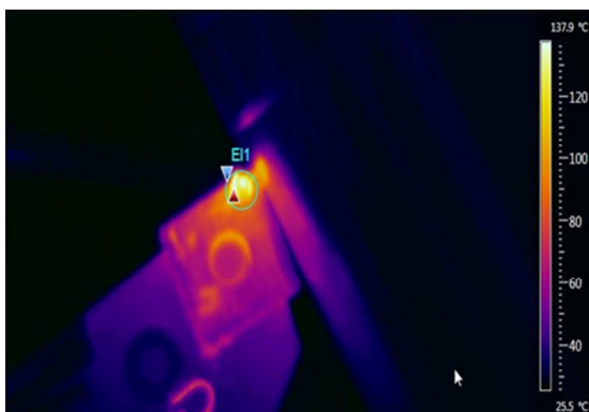


Fig. 16. Thermogram for Vc = 112m/min, a = 0.14 mm/rev, and P = 1 mm.

V. OPTIMIZATION OF CUTTING CONDITIONS

This goal can be achieved by intervening in the different stages of the production of the part:

- Design of the assembly to be manufactured.
- Part definition.
- Choice of manufacturing range.
- Choice of cutting conditions.

Cutting conditions can be optimized by setting an optimum cutting temperature obtained during experimentation. It can be given by the manufacturer depending on the technical characteristics of the pad. In this paper, a method is proposed to find the optimal cutting conditions. The choice of cutting conditions has a direct impact on the machining time of the part, therefore on the cost price of machining and on the productivity improvement. The optimization plot allows us to interactively modify the cut parameters of the input variables to perform sensitivity analysis and possibly improve the initial solution. We apply the optimization technique of the Minitab software used in the current work, for the measurement just after the release of the tool and under the following machining constraints:

$$78 \leq Vc \leq 220; \quad 0.08 \leq a \leq 0.2; \quad 0.25 \leq p \leq 1 \quad (3)$$

By choosing a temperature of 100° we obtained the results of the optimized input variables grouped in Table IV.

TABLE IV. OPTIMIZED CONDITIONS

Solution	T°				Desirability
	Vc	a	p	Fit	
1	149	0.14	0.348485	99.967	0.999446
2	220	0.185560	0.256348	100.148	0.997301
3	78	0.150854	0.991703	103.348	0.939131

For desirability index equal to 0.999446, the optimal conditions are: Vc=149m/min, a=0.14mm/rev, p=0.34 mm. The optimization diagram in Figure 17 shows the influence of the cutting conditions with the fixed cutting temperature.



Fig. 17. Impact of cutting conditions.

VI. CONCLUSION

This work shows that a thermography technique is a useful procedure for establishing an experimental methodology for evaluating cutting temperature during the machining operations. It is therefore a method of mapping temperatures in real time, allowing the evaluation over time of surface thermal phenomena. The advances in manufacturing technology require us to estimate and predict the temperature rise at different points of the workpiece-tool interface in order to optimally adjust different parameters beforehand to improve machinability.

No previous research work has used only an infrared camera. The major difficulty in taking the machining sequence by the camera is the rolling of the chip, hence the need to choose the cutting conditions well and to have good protection and fixing. The experimental results allow us to conclude that the variations of the temperatures are very weak in permanent regimes for invariant cutting parameters, that the stresses applied by the tool on the machined material lead to a rise in temperature and that the heat flow generated during machining is largely evacuated by the chip. The experiments allowed us to determine the temperatures of the machined surface of the part as well as that of the cutting edge for different cutting parameters. The fit of the model was checked and found to be adequate at an accuracy level of 88.87% for temperature measurements just after tool release. This demonstrates that the model can be used to predict the cutting temperature. The technique could be an economical and effective method for temperature prediction and optimization of the cutting parameters.

The quality of the parts produced depends largely on the cutting conditions and this quality is an important parameter during the production of mechanical parts. The cutting fluid is

also an important parameter since it allows to limit the rise in temperature in the cutting zones and to establish the presence of a fluid film between the different surfaces. However, in order to protect the environment and the health of the personnel, the current trend is to limit and even eliminate the use of cutting fluids.

REFERENCES

- [1] S. K. Choudhury and P. Srinivas, "Tool wear prediction in turning," *Journal of Materials Processing Technology*, vol. 153–154, pp. 276–280, Nov. 2004, <https://doi.org/10.1016/j.jmatprotec.2004.04.296>.
- [2] J.-T. Horng, N.-M. Liu, and K.-T. Chiang, "Investigating the machinability evaluation of Hadfield steel in the hard turning with Al₂O₃/TiC mixed ceramic tool based on the response surface methodology," *Journal of Materials Processing Technology*, vol. 208, no. 1, pp. 532–541, Nov. 2008, <https://doi.org/10.1016/j.jmatprotec.2008.01.018>.
- [3] O. B. Abouelatta and J. Mádl, "Surface roughness prediction based on cutting parameters and tool vibrations in turning operations," *Journal of Materials Processing Technology*, vol. 118, no. 1, pp. 269–277, Dec. 2001, [https://doi.org/10.1016/S0924-0136\(01\)00959-1](https://doi.org/10.1016/S0924-0136(01)00959-1).
- [4] I. Mukherjee and P. K. Ray, "A review of optimization techniques in metal cutting processes," *Computers & Industrial Engineering*, vol. 50, no. 1, pp. 15–34, May 2006, <https://doi.org/10.1016/j.cie.2005.10.001>.
- [5] P. J. T. Conradie, G. A. Oosthuizen, N. F. Treurnicht, and A. A. Shaalane, "Overview of Work Piece Temperature Measurement Techniques for Machining of Ti6Al4V#," *The South African Journal of Industrial Engineering*, vol. 23, no. 2, 2012, <https://doi.org/10.7166/23-2-335>.
- [6] N. M. M. Reddy and P. K. Chaganti, "Investigating Optimum SiO₂ Nanolubrication During Turning of AISI 420 SS," *Engineering, Technology & Applied Science Research*, vol. 9, no. 1, pp. 3822–3825, Feb. 2019, <https://doi.org/10.48084/etasr.2537>.
- [7] A. R. Motorcu, Y. Isik, A. Kus, and M. C. Cakir, "Analysis of the cutting temperature and surface roughness during the orthogonal machining of AISI 4140 alloy steel via the Taguchi method," *Materiali in tehnologije*, vol. 50, no. 3, pp. 343–351, Jun. 2016, <https://doi.org/10.17222/mit.2015.021>.
- [8] A. Kus, Y. Isik, M. C. Cakir, S. Coşkun, and K. Özdemir, "Thermocouple and Infrared Sensor-Based Measurement of Temperature Distribution in Metal Cutting," *Sensors*, vol. 15, no. 1, pp. 1274–1291, Jan. 2015, <https://doi.org/10.3390/s150101274>.
- [9] N. A. Abukhshim, P. T. Mativenga, and M. A. Sheikh, "Heat generation and temperature prediction in metal cutting: A review and implications for high speed machining," *International Journal of Machine Tools and Manufacture*, vol. 46, no. 7, pp. 782–800, Jun. 2006, <https://doi.org/10.1016/j.ijmactools.2005.07.024>.
- [10] I. Korkut, M. Boy, I. Karacan, and U. Seker, "Investigation of chip-back temperature during machining depending on cutting parameters," *Materials & Design*, vol. 28, no. 8, pp. 2329–2335, Jan. 2007, <https://doi.org/10.1016/j.matdes.2006.07.009>.
- [11] N. Benhadji Serradj, "Contribution to the evaluation of the thermal field at the tool-part interface for the optimization of machining conditions," Ph.D. dissertation, University of Tlemcen, Tlemcen, Algeria, 2022.
- [12] N. B. Serradj, A. D. K. Ali, and M. E. A. Ghernaout, "A Contribution to the Thermal Field Evaluation at the Tool-Part Interface for the Optimization of Machining Conditions," *Engineering, Technology & Applied Science Research*, vol. 11, no. 6, pp. 7750–7756, Dec. 2021, <https://doi.org/10.48084/etasr.4235>.
- [13] M. PradeepKumar, K. Amarnath, and M. SunilKumar, "A Review on Heat Generation in Metal Cutting," *International Journal of Engineering and Management Research*, vol. 5, no. 4, pp. 193–197, Aug. 2015.
- [14] O. Riou, P.-O. Logerais, and J.-F. Durastanti, "Quantitative study of the temperature dependence of normal LWIR apparent emissivity," *Infrared Physics & Technology*, vol. 60, pp. 244–250, Sep. 2013, <https://doi.org/10.1016/j.infrared.2013.05.012>.
- [15] N. M. M. Reddy and P. K. Chaganti, "Investigating Optimum SiO₂ Nanolubrication During Turning of AISI 420 SS," *Engineering, Technology & Applied Science Research*, vol. 9, no. 1, pp. 3822–3825, Feb. 2019, <https://doi.org/10.48084/etasr.2537>.
- [16] D. Kara Ali, N. Benhadji Serradj, and M. E. A. Ghernaout, "Qualification and Validation of an in-situ Measurement Method of the Machining Temperature," in *Mechanism, Machine, Robotics and Mechatronics Sciences*, Cham, 2019, pp. 15–27, https://doi.org/10.1007/978-3-319-89911-4_2.
- [17] *FLIR SC325*. FLIR Systems, 2010.